International Journal of Integrated Engineering, Vol. 3 No. 1 (2011) p. 1-4

Numerical Analysis of Auto-ignition of Ethanol

Vaibhav Kumar Sahu[1], Shrikrishna Deshpande[1], Vasudevan Raghavan[1,*]

[1]Department of Mechanical Engineering
Indian Institute of Technology Madras, Chennai 600036, INDIA.

Received 28 June 2011; accepted 5 August 2011, available online 24 August 2011

Abstract: Renewable and alternative fuels such as ethanol find application in several combustion devices. Fundamental characteristics of these fuels in terms of ignition and burning rate are to be understood in order to use them in these applications. In this study, a numerical analysis of auto ignition characteristics of ethanol is presented. Opposed flow configuration, in which fuel and nitrogen emerges from the bottom duct and hot air flows down from the top duct, has been employed. Commercial CFD software FLUENT is used in the simulations. Global single step mechanism is used to model kinetics. For various mass fractions of fuel, the air temperature at which auto-ignition occurs has been recorded. The numerical results are compared with the experimental data available in literature.

Keywords: Renewable fuel, ethanol, numerical simulation, auto ignition, single-step mechanism

1. Introduction

Ethanol is the most effective bio-fuel. Its easier production from agricultural feed-stocks, sugar cane and Fischer-Tropsch method makes it dominant among other bio-derived fuels. It can be employed directly for engine application, both from the point of view of developing renewable fuels for energy needs in future and to address the environmental issues such as exhaust emissions and global warming. For these relatively new bio-fuels, fundamental studies in terms of burning characteristics are done in several configurations [1]. The conditions at which bio-fuel auto-ignites should be understood thoroughly to reveal the combustion performance with better efficiency. Numerical simulation including global single-step chemistry in oxidative environment is useful where the study in detailed chemistry is expensive. The chemical kinetics of gas phase oxidation of ethanol has been reported over last five decades.

Data have been reported from nonflow reactors, flow reactors, diffusion flames, and laminar premixed flames experiments by several researchers [2-5]. Detailed chemical kinetics models to describe the gas-phase oxidation of ethanol in air are available in literature [6]. Apart from that a global single step mechanism for ethanol oxidation is also available [7]. Experimental studies have been reported on extinction and autoignition of methanol and ethanol flames in laminar, non uniform flows for both non premixed and premixed flames in counter-flow configuration by Seiser et al. [8].

Numerical investigations in this paper are performed for non-premixed laminar counter-flow flame using global single step kinetics as reported in Dubey et al. [9]. The focus of present numerical study is to further validate the single-step reaction kinetics using the available experimental data. Numerical investigation has been done for the critical conditions of auto-ignition against various strain rates and mass fractions.

2. Numerical Model

In the present study, a comprehensive combustion model has been developed using commercial CFD software, FLUENT 6.3. The salient features of the numerical combustion model include temperature and concentration dependent thermo-physical properties such as density, specific heat, thermal conductivity and viscosity, multi-component mass diffusion, single-step chemical kinetics mechanism. Appropriate model parameters available in FLUENT has been chosen. The effect of normal gravity has also been included in the model. The mass, momentum and species conservation equations are solved along with energy equation. The energy equation for two dimensional, steady, axisymmetric and laminar reactive flows can be written as follows:

$$\nabla \cdot (\rho v T) = \nabla \cdot \left(\frac{k}{c_p} \nabla T \right) + \frac{k}{c_p^2} \nabla T \cdot \nabla c_p - \frac{1}{c_p} \sum_{i=1}^{N} \rho Y V_i \cdot \nabla h_i - \frac{1}{c_p} \sum_{i=1}^{N} \omega_i h_i \qquad (1)$$

In equation (1), T is the temperature; k, c_p and ρ are mixture thermal conductivity, specific heat and density, respectively, and V_i, ω_i and h_i, are the diffusion velocity, net rate of production and absolute enthalpy of i^{th} species, respectively. A Finite Volume Method based approach along with suitable upwind scheme for convection terms and SIMPLE type algorithms for velocity pressure coupling, is employed for discretizing the above governing equations. Appropriate second order accurate solution techniques have been employed for solving the discretized equations.

*Corresponding author: raghavan@iitm.ac.in

2.1 Numerical Domain

In the axisymmetric model, the computational domain is as shown in Fig. 1. A domain with extents of 12 mm in the axial direction and 25 mm in the radial direction is chosen. A commercially available meshing software called GAMBIT 2.0 has been employed to create the computational domain and for generating grid.

2.2 Boundary conditions

i. Fuel Inlet: At the fuel inlet boundary, velocity profile of the fuel jet is specified. Fully developed velocity profile is prescribed such that the flow rate corresponding to the experimental value is obtained. This velocity is calculated for corresponding strain rate. A constant temperature of 298 K is prescribed. Mass fraction value of fuel is prescribed corresponding to the experimental conditions.

ii. Oxidizer Inlet: This boundary is treated in the same manner as that of fuel inlet boundary. The mass fraction of oxygen is 0.232. Velocity profile corresponding to that of oxidizer flow rate has been specified. Oxidizer velocity is also calculated for corresponding strain rate. Temperature of oxidizer has been increased from 298 K to critical temperature of autoignition.

iii. Pressure Outlet: At the exit boundary, flow leaves to the atmosphere. Due to buoyancy driven flow, incoming flow can also occur at this boundary at a few cells. Therefore, a pressure outlet condition, which drives the flow with respect to local pressure gradient, has been chosen at this boundary. In case of back-flow into the domain oxygen mass fraction of 0.232 and a constant temperature of 300 K are specified, representing the ambient air.

iv. Axis: This boundary represents the centerline of the burner. For this axisymmetric problem, an axis boundary condition has been specified (Fig. 1). At this boundary, the boundary conditions specified are $v_r = 0$ and $\frac{\partial}{\partial r}(\varphi) = 0$, where φ is any other variable.

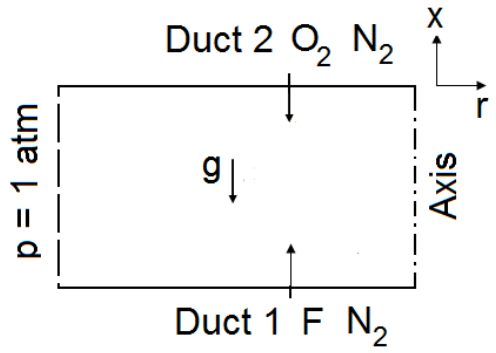

Fig. 1 Computational domain with boundary types.

To characterize the boundary velocities and to compare between experimental and numerical results, we define a quantity called Strain rate (a_2) in the region between the stagnation plane and duct 2. It is just a quantity used to characterize the flow-field irrespective of the actual strain experienced by the flame [8], and is given by,

$$a_2 = \frac{2|V_2|}{L}\left(1 + \frac{|V_1|}{|V_2|}\sqrt{\frac{\rho_1}{\rho_2}}\right) \quad (2)$$

In the experiments and numerical calculations, the momentum values of the counter-flowing reactant streams $\rho_i V^2_i$; i = 1; 2 at the boundaries are kept equal to each other. Here, ρ represents the density. Subscripts 1 and 2 are used to denote the values of various quantities at the exit of their corresponding ducts. This condition ensures that the stagnation plane formed by the two streams is approximately in the middle of the region between the two ducts.

2.3 Mesh generation

The domain has been divided in to several quadrilateral control volumes. Multi-block structured grids are used with uniform spacing in the radial and axial directions. After carrying out grid independence study, the domain with 250 cells in the radial direction and 240 grids in the axial direction has been chosen for all the cases in this study.

2.4 Numerical Procedure

As mentioned earlier, the governing equations involving conservations of species, mass, momentum and energy equations are solved using FLUENT, which employs Finite Volume Method. The steady-state equations have been solved in a segregated manner with double precision accuracy. A second order upwind scheme is used for convective terms. A laminar species transport model with volumetric reactions is used along with finite rate chemistry. Full multi-component diffusion along with a diffusion energy source is used to model the species diffusion. A global single-step reaction for ethanol oxidation is used to model finite rate reaction chemistry. The reaction is given by

$C_2H_5OH + 3O_2 + 11.28N_2 \rightarrow 2CO_2 + 3H_2O + 11.28N_2$ Molar

based reaction rate ($\bar{\dot{\omega}}$ in $kmol/m^3s$) for the above ethanol air oxidation is taken from Dubey et al.[9] as

$$\bar{\dot{\omega}} = 1.55 \cdot 10^{10} \exp\left(\frac{-1.256 \cdot 10^8}{8314.3 \cdot T}\right) \cdot [C_2H_5OH]^{n_1}[O_2]^{n_2} \quad (3)$$

Arrhenius rate equation is used to obtain the rate of formation/destruction of all the species. The net rates of formation of several species participating in the chemical reaction have been solved simultaneously using a stiff chemistry solver. Thermo-physical properties of the species have been calculated as functions of temperature and species concentration. The properties of each species as a function of temperature have been calculated using kinetic theory. Viscosity, binary mass diffusivity between

any two species and thermal conductivity are calculated using kinetic theory. Specific heat capacities are calculated using temperature dependent piecewise polynomial functions. For the mixture, density is calculated using mixture molecular weight and ideal-gas equation of state, specific heat capacity using the mixing law, viscosity and thermal conductivity using ideal gas mixing law.

2.5 Solution procedure

The velocity, temperature and species mass fractions are initialized to some constant values across the computational domain. At a given strain rate and oxidizer temperature $T_2<T_{2,I}$ flow field is established. Here $T_{2,I}$ is the temperature of air at autoignition. Temperature of air, T_2 is gradually increased until autoignition takes place. Only those cases where autoignition takes place close to the axis of symmetry are recorded as valid data points. Appropriate under-relaxation factors are set for pressure, density, body force, momentum, species and temperature. The case is executed till convergence is obtained. The convergence criterion for all the equations is that the difference between the current and the previous iteration value is below $1x10^{-6}$.

3. Results and Discussion

Critical conditions for autoignition of non-premixed ethanol flames are shown in Figs. 2 and 3. Fig. 2 shows the temperature of air at autoignition as a function of mass fraction of fuel at the fuel duct exit. The data is obtained at a fixed value of strain rate a_2 = 300 s^{-1}. Measured values of Seiser et al. [8] agree well with the numerical calculations as shown in Fig. 2.

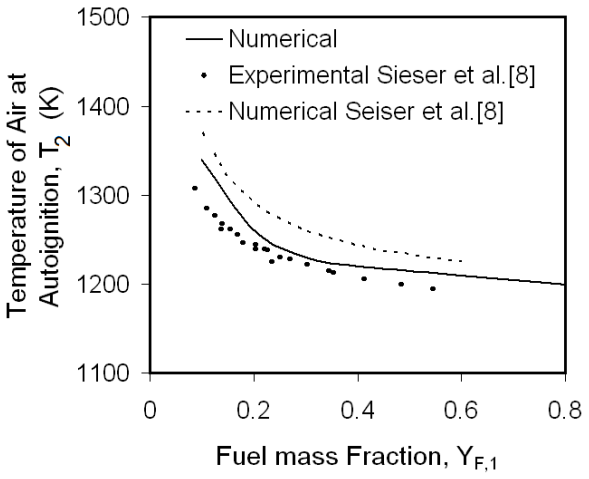

Fig. 2 Numerical data showing the temperature of Air at autoignition as a function of the fuel mass fraction $Y_{F,1}$, at a fixed strain rate of a_2=300 s^{-1} compared with Seiser et al. [8] Experimental and Numerical data.

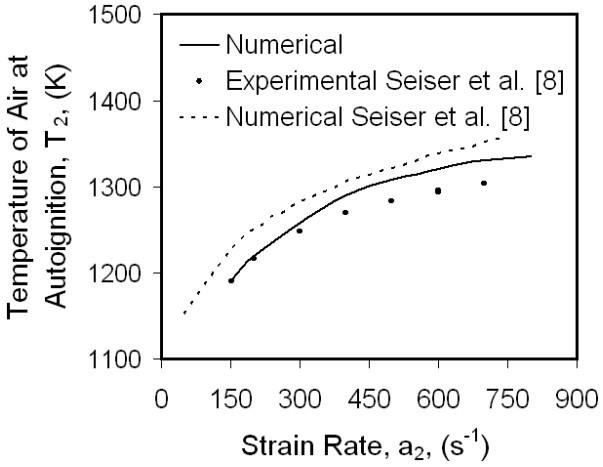

Fig. 3 Numerical data showing the temperature of Air at autoignition as a function of the strain rate, at a fixed mole fraction, $X_{F,1}$=0.15 compared with Seiser et al. [8] Experimental and Numerical data.

Fig. 3 shows the temperature of air at autoignition, $T_{2,I}$, as a function of the strain rate. The numerical data in Fig. 3 is obtained with mole fraction of fuel, $X_{F,1}$ = 0.15. At a given strain rate autoignition will take place for values of air temperature larger than $T_{2,I}$. The value of $T_{2,I}$ increases with increasing strain rate.

The predictions by the present numerical model (Figs. 2 and 3) are quite close to the experimental results than the detailed chemical kinetics predictions by Seiser et al. [8]. This is probably due to the capabilities of the numerical models used in the present study as compared to that in the reported work [8]. Also, the error accumulation in detailed mechanism would be more than that in single-step mechanism if not properly resolved.

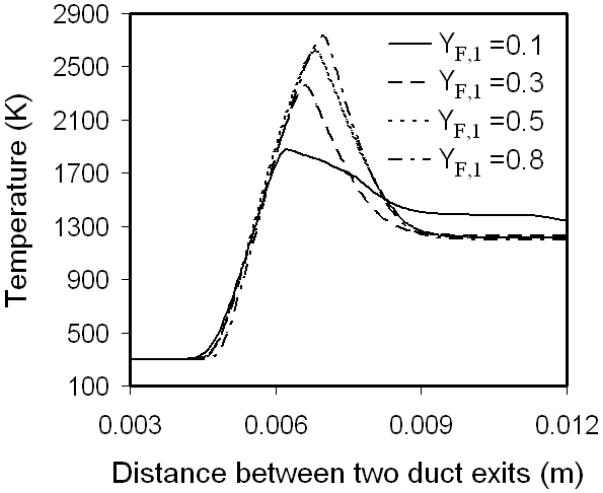

Fig. 4 Numerically obtained temperature profiles plotted at axis of symmetry between two duct exits for different mass fractions of fuel at a constant strain rate a_2 = 300 s^{-1} when autoignition occurs.

Fig. 4 shows temperature profiles for different mass fractions of fuel plotted at axis of symmetry, for constant

strain rate a_2 = 300 s^{-1}, when auto ignition occurs. It is clear from the Fig. 4 that as the mass fraction of fuel increases the temperature peak also increases. The rate of increase, however, is not linear and plateaus after the mass fraction value greater than around 0.5.

Table 1 presents the numerically obtained maximum temperature data for different fuel mass fractions and different air temperatures at auto ignition. The adiabatic flame temperature for each fuel mass fraction and hot air temperature is also calculated and listed. As the fuel mass fraction increases at a given strain rate, the adiabatic and maximum temperatures increases in non-linear fashion. The air temperature, at which auto ignition occurs, decreases with increasing fuel mass fraction due to enhanced heat release rate. Table 1 also indicates that the maximum temperature and calculated adiabatic flame temperature are close. This ensures correct autoignition temperature has taken predicted by the numerical model by systematically varying the hot air temperature for all the cases.

Table 1 Numerically obtained maximum flame temperature for different fuel mass fraction and air temperature at constant strain rate a_2=300 s^{-1} and adiabatic flame temperature for corresponding reaction.

Fuel mass fraction ($Y_{F,1}$)	Tempera-ture of hot air T_2 (K)	Maximum flame tempera-ture (K)	Adiabatic Flame tempera-ture (K)
0.1	1340	1880	1908
0.3	1230	2364	2541
0.5	1215	2627	2740
0.8	1200	2735	2882

4. Summary

Results of numerical analysis of autoignition of non-premixed ethanol flames have been reported in detail. Using experimental measurements reported in Seiser et al. [8], validation of numerical model using single step kinetics has been carried out. Numerical predictions of autoignition temperatures are quite close to the experimental observations. This ensures that the numerical model along with single-step kinetics sub-model is capable of prediction the onset of ignition quite well. Numerical results also show that temperature of air at autoignition is a function of strain rate and fuel mass fraction.

References

[1] Agarwal, A.K. Biofuels (alcohols and biodiesel) applications as fuels for internal combustion engines. *Progress in Energy Combustion science*, Volume 33, (2007), pp. 233-271.

[2] Dunphy, M.P., Patterson, P.M., and Simmie, J.M. High temperature oxidation of ethanol. Part 2-Kinetic modeling. *Journal of Chemical Society. Faraday Transactions,* Volume 87, (1991), pp. 2549-2560.

[3] Egolfopoulos, F.N., Du, D.X., and Law, C.K. A study on ethanol oxidation kinetics in laminar premixed flames, flow reactors and shock tubes. *Procceeding of Combustion Institute*, Volume 24, (1992), pp. 833-841.

[4] Saxena, R., and Williams, F.A. Numerical and experimental studies of ethanol flames. *Proceedings of Combustion Institute*, Volume 31, (2007), pp. 1149-1156.

[5] Nortan, T.S., and Dryer, F.L. An Experimental and modeling study of ethanol oxidation kinetics in an atmospheric pressure flow reactor. *International Journal of Chemical Kinetics*, Volume 24, (1992), pp. 319-344.

[6] Marinov, N.M. A detailed chemical Kinetic model for high temperature ethanol oxidation. *International Journal of Chemical Kinetics*, Volume 31, (1999), pp. 183-220.

[7] Westbrook, C.H., and Dryer, F.L. Simplified reaction mechanisms for the oxidation of hydrocarbon fuels in flames. *Combustion Science and Technology*, Volume 27, (1981), pp. 31-43.

[8] Seiser R., Humer S., Seshadri K., and Pucher E. Experimental investigation of methanol and ethanol flames in non-uniform flows. *Proceedings of Combustion Institute*, Volume 31, (2007), pp. 1173-1180.

[9] Dubey, R., Bhadraiah, K., Raghavan, V., On the Estimation and Validation of Global Single-Step Kinetics Parameters of Ethanol-Air Oxidation Using Diffusion Flame Extinction Data. *Combustion Science and Technology*, Volume 183, (2011), pp. 43-50.